IOPscience iopscience.iop.org

Home Search Collections Journals About Contact us My IOPscience

Gamma-ray sensor based on an iron chloride tetraphenyl porphyrin/p-silicon heterojunction diode

This article has been downloaded from IOPscience. Please scroll down to see the full text article.

2012 Phys. Scr. 86 065801

(http://iopscience.iop.org/1402-4896/86/6/065801)

View the table of contents for this issue, or go to the journal homepage for more

Download details:
IP Address: 193.227.50.69
The article was downloaded on 01/12/2012 at 13:31

Please note that terms and conditions apply.

Phys. Scr. **86** (2012) 065801 (8pp) doi:10.1088/0031-8949/86/06/065801

Gamma-ray sensor based on an iron chloride tetraphenyl porphyrin/p-silicon heterojunction diode

H M Zeyada[1], M I El-Gammal[2], O A ElBatrawy[2] and B M Omar[2]

[1] Department of Physics, Faculty of Science at New Damietta, University of Damietta, 34517 Damietta, Egypt
[2] Department of Environmental Sciences, Faculty of Science at New Damietta, University of Damietta, 34517 Damietta, Egypt

E-mail: hzeyada@gmail.com

Received 31 October 2011
Accepted for publication 6 November 2012
Published 30 November 2012
Online at stacks.iop.org/PhysScr/86/065801

Abstract
An Au/Fe(III)ClTPP/p-Si/Al heterojunction diode was constructed. The *I–V* characteristics of the sensor under dark and illumination conditions were studied before and after γ-irradiation. *C–V* measurements were also carried out at 1 MHz before and after γ-irradiation. Two conduction mechanisms are operating in the device depending on the applied potential. Thermionic emission conduction is operating up to 0.6 V and space charge limited current conduction is operating at voltages >0.6 V. The rectification ratio, built-in potential and density of defect states in the interfacial layer increase with increasing the irradiation dose. Increasing the irradiation dose decreases the quality factor, the dark current, the capacitance at zero bias potential and the carrier density in the depletion region. These changes are attributed to an increase in the density of defect states in the interfacial layer and energy gap of a semiconductor upon γ-irradiation.

PACS numbers: 85.30.Hi, 85.30.Kk, 73.30.+y

(Some figures may appear in colour only in the online journal)

1. Introduction

The bilayer devices, which are based on organic/inorganic layers, overcome the disadvantages of single-layer devices. Organic thin films introduce a dipole layer at the semiconductor organic interface and thus change the Schottky barrier height, which could be increased or decreased depending on the conduction type of the organic semiconductor [1].

The fundamental device parameters can be controlled by means of the choice of organic molecule and the interlayer thickness. Iron(III) chloride tetraphenylporphyrine is a typical porphyrin compound. The molecular structure of Fe(III)ClTPP is shown in figure 1. It is a π-conjugated electron system. Thin films of the π-conjugated electron system have many technological applications such as nonlinear optical materials [2, 3], chemical sensors for volatile organic compounds [4] and information storage [5]. Porphyrin and its derivatives are distinguished by their synthetic versatility, thermal stability and large π-electron system, photochemical and unique opto-electrical properties. Therefore, their thin films are applied in many technological devices including: solar cells [6, 7], information storage [5], molecular wire [8] and nonlinear optical materials [2, 3]. The optical properties of iron(III) chloride tetraphenylporphyrine thin films have been investigated [9, 10]. The molar extinction coefficient of Fe(III)ClTPP shows an extremely high molar extinction coefficient of 7.5×10^4 cm^2 mol^{-1} and a broad absorption band in the wave number range of 500–5000 cm^{-1} [9]; this result is comparable with those of organic dyes. A high molar extinction coefficient and a broad absorption band are required in materials to increase the photocurrent density and solar conversion efficiency [11].

The effects of γ-irradiation on electrical properties of devices are of scientific interest and technological importance. Exposure may cause strong electrical and

 © 2012 The Royal Swedish Academy of Sciences

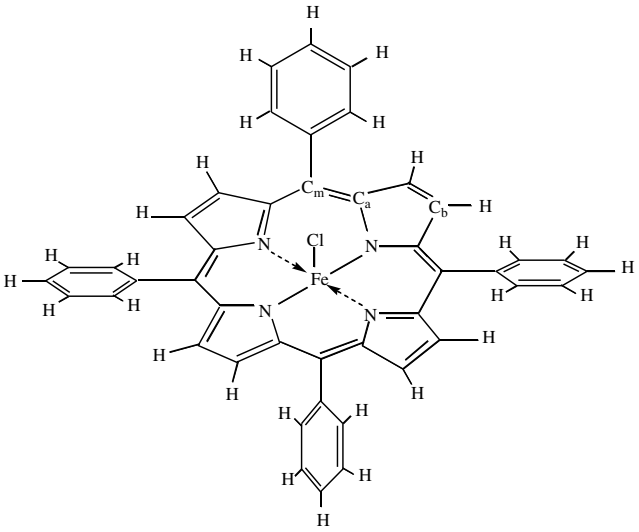

Figure 1. Molecular structure of Fe(III)ClTPP.

dielectric changes in organic/inorganic devices. In addition, the main material forming organic/inorganic devices have different sensitivity to γ-irradiation. Depending on the energy of irradiation, structural defects such as vacancies, interstitials, defect complexes and amorphization are created by low-energy radiation. High-energy radiation penetrates the organic/inorganic interface and results in recombination centers that act as minority/majority carrier trapping centers [12, 13]. γ-irradiation creates defects in the band gap which affects the free carrier concentration and leads to an increase or decrease in the barrier height in p-type and n-type semiconductors, respectively [14].

In this work, we report on the electrical characteristics of an Au/Fe(III)ClTPP/p-Si/Al heterojunction device before and after exposure to γ-ray doses of 1 and 1.25 kGy. The capacitance–voltage (C–V) and current–voltage (I–V) measurements were made with the purpose of determining fundamental parameters of the device such as: the ideality factor, barrier height, width of depletion region, carrier concentration at the edge of the depletion region, variation of capacitance with bias potential and density of defect states in the interfacial layer and their dependence on the irradiation dose.

2. Experimental details

5, 10, 15, 20-Tetraphenyl-21H, 23H-porphyrin iron (III) chloride (Fe(III)ClTPP) was purchased from Sigma-Aldrich and was used in as-received condition without further purification. The device was prepared using a polished p-type Si wafer with [100] orientation and a hole concentration of 1.6×10^{23} m^{-3} with a thickness of 400 μm. In order to remove the native oxide from the surface of p-Si, the substrate was etched by CP4 solution (HF:HNO_3:CH_3COOH in the ratio of 1 : 6 : 1) for 10 s and then rinsed with deionized water and dried. A thin film of Fe(III)ClTPP with a thickness of 80 nm was deposited on to the etched front surface of Si wafer by the conventional thermal evaporation technique. The thick gold electrode in the form of a network was thermally deposited on an Fe(III)ClTPP film. The back contact was manufactured by depositing a relatively thick Al film on to the bottom of the p-Si substrate. Au and Al were selected as electrodes since they make Ohmic contacts with Fe(III)ClTPP and Si, respectively. Those electrodes are an infinite reservoir of charge and can maintain a steady-state space charge limited current (SCLC) in the device [15]. A high-vacuum coating unit (Edwards Model E306A, UK) was used. Thin films were vacuum deposited onto optical flat quartz substrates for absorbance measurements and onto optical flat KBr substrates for Fourier transform infrared spectroscopy (FTIR) measurements. A quartz crucible source heated by a tungsten coil in a vacuum of 10^{-4} Pa was used as an evaporator for Fe(III)ClTPP. Au and Al films were evaporated individually using a tungsten filament. The substrate temperature was kept at room temperature during the deposition process. The deposition rate was controlled at 3 nm s^{-1} using a quartz crystal thickness monitor (Model TM-350, Maxtech, Inc., USA), and the thickness of films was determined accurately after deposition using a multiple beam interferometer [16]. The as-manufactured device has been exposed to different doses of γ-ray. The γ-ray doses were obtained from a Technetium-99m generator (Bristol-Myers Squibb Pharma Belgium) and are in the range of 1–1.25 kGy.

Infrared spectroscopy on Fe(III)ClTPP in powder form and as deposited thin films was performed. A Perkin-Elmer infrared spectrophotometer (model 887) was used for this purpose; 1 mg of Fe(III)ClTPP powder was mixed with 49 mg of vacuum dried IR-grade KBr and compressed by a hydraulic press under a pressure of 10 tons cm^{-2} at room temperature to form pellets. The thickness of each pellet is about 1 mm and the area is about 25 mm^2. Thin films of Fe(III)ClTPP with a thickness of 300 nm were deposited onto optically flat KBr single-crystal substrates kept at room temperature.

The transmittance, $T(\lambda)$, spectra of the film was measured at nearly normal incidence of light in the spectral range of 200–2500 nm using a double-beam spectrophotometer (Jasco model V-570 UV–vis–NIR). For deposited films, the measurements obtained by this spectrophotometer gave an uncertainty of 1%. A quartz blank substrate identical to that used for the thin film deposition was used as the reference for the transmission scan. The absorbance of the film was calculated from the relation $A = \mathrm{Log}_{10}(1/T)$.

The sensor was designed as shown schematically in figure 2. The current–voltage (I–V) measurements of the device at different doses of γ-ray irradiation were measured in dark condition by using stabilized power supply and a high impedance electrometer (Keithley Model 617A). In the case of illumination, the incident light from a tungsten filament lamp falls normally on the device from the Au grid side. The intensity of incident light was recorded by a calibrated digital light meter (Lutron-Model LX-107) situated at the same level position of the device and is calculated as 20 mW cm^{-2}. The temperature of the device was fixed at room temperature during measurements. The room temperature capacitance–voltage (C–V) measurements of Au/Fe(III)ClTPP/p-Si/Al device after being exposed to different doses of irradiation were made at 1 MHz by using a computerized C–V meter (Model 4108, Solid State Measurements, Inc., Pittsburgh, PA) in air and in dark conditions.

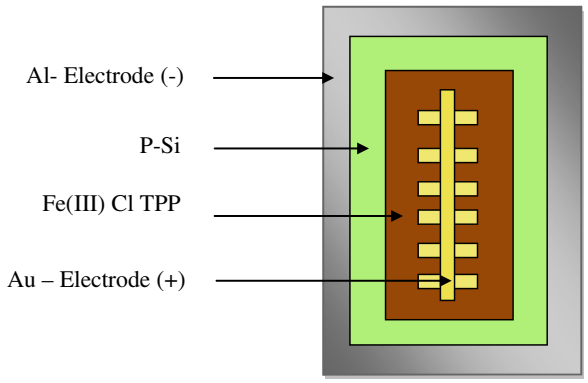

Figure 2. Schematic diagram of the Au/Fe(III)ClTPP/p-Si/Al device.

3. Results and discussion

The structural analysis has been performed by the scanning electron microscope and X-ray diffraction techniques on Fe(III)ClTPP in powder form and in thin film conditions (as deposited, annealed and γ-ray irradiated films). Our group [9, 10] has published the results previously. The results revealed that Fe(III)ClTPP is polycrystalline structure in powder form and has nanocrystallite in thin film conditions.

The FTIR transmittance spectra of Fe(III)ClTPP in powder form and as-deposited film are depicted in figure 3. The assignment of transmission peaks was done by the method of [17] and is illustrated in table 1. The transmission peaks in the fingerprint region (500–1500 cm^{-1}) of Fe(III)ClTPP are identical in all cases. The results of FTIR spectroscopy indicate that there is no change in molecular bonds of Fe(III)ClTPP upon thermal deposition.

The optical absorption spectra for as-deposited Fe(III)ClTPP thin film is illustrated in figure 4. The spectra show an intense absorption band in the wavelength range of 417–452 nm termed the Soret band (B) with its Davidov splitting and three additional weaker absorption bands termed Q-bands closely over the wavelength range of 500–700 nm. The B- and Q-bands are weaker and less sharp than those of the corresponding ones of TPP [7]. This may be ascribed to the incorporation of FeCl atoms in the central cavity of TPP. The absorption spectra of Fe(III)ClTPP is characterized by a broad absorption band extending in the wavelength range of 300–500 nm. A broad absorption band is required in materials to increase the photocurrent density and solar conversion efficiency. The type of electronic transition and the value of energy gap have been determined [9, 10]. It has been shown that direct and indirect transitions occur in as-deposited and irradiated films. The direct band gaps for the as-deposited film were found to be 1.7 and 2.63 eV for onset and optical band gap, respectively, and 1.65 and 2.63 eV for onset and optical band gap in the irradiated films [9]. The values of indirect energy gaps were found to be 1.5 and 2.43 eV for onset and optical band gap, respectively, in the as-deposited films and 1.36 and 2.43 eV for onset and optical band gap in irradiated films [9]. In their opinion, indirect transition rather than direct transition occur in Fe(III) Cl TPP films [9].

Figure 5 illustrates the junction capacitance (C_J) of a diode as a function of the reverse bias voltage (V_r). C_J decreases when V_r was increased. At a fixed V_r, C_J is greater for the as-fabricated device than that for the irradiated one. Table 2 gives the zero bias junction capacitance (C_{J0}) for as-fabricated and γ-irradiated diodes.

Figure 6 is a plot of $1/C_J^2$ versus V_r; it shows a straight line and this indicates the formation of a one-sided abrupt junction. The slope gives the acceptor concentration (N_s) of the Fe(III)ClTPP and the intercept (at $1/C_J^2 = 0$) gives the built-in potential V_{bi}. For one-sided abrupt junctions the capacitance per unit area is given by [18]

$$\frac{1}{C^2} = \frac{2(\varepsilon_{si}N_{si} + \varepsilon_s N_s)}{q\varepsilon_{si}\varepsilon_s N_{si}N_s}(V_{bi} \pm V), \qquad (1)$$

where ε_{si} is the dielectric constant of Si, ε_s is the dielectric constant of Fe(III)ClTPP, N_{si} refers to the acceptor density in Si and N_s stands for acceptor density in Fe(III)ClTPP. The $\pm$ signs are for the reverse and forward-bias conditions, respectively. By substituting for ε_{si} as 11.9, ε_s as 4 and the hole concentration in Si wafer as 1.6×10^{23} m^{-3} in equation (1), we can deduce the built-in voltage and the acceptor concentration, N_s. Table 2 lists the results on the capacitance of the device, C_{JO}, at zero bias potential, built-in voltage and acceptor concentration, N_s. The values of C_{JO} and N_s decrease with an increase in irradiation dose and the built-in potential increases with increasing the irradiation dose.

The origin of the rectification behavior of the Au/Fe(III)ClTPP/p-Si/Al device can be understood by assuming that the organic/inorganic contact acts as a heterojunction between Fe(III)ClTPP (nearly intrinsic semiconductor) and a lightly doped Si. The rectifying junction is then formed by the energy offset between the frontier orbital of the Fe(III)ClTPP and the conduction or the valence band minima of Si. The Fermi energy of Fe(III)ClTPP was almost completely determined by the density of charge carriers injected from the metal contact on its surface or across the Fe(III)ClTPP/Si heterojunction. The movement of the quasi-Fermi energy from its mid-energy gap position could also result in a change in the energy level offset at the Fe(III)ClTPP/Si heterojunction interface—possibly allowed to shift its position by an intervening oxide layer residing on the Si surface [19]. El-Nahass *et al* [19] proposed an energy level diagram of the Fe(III)ClTPP/Si heterojunction diode under thermal equilibrium. They showed that application of positive potential to the Si steers the holes from the Si to the Fe(III)ClTPP; this results in the bending of the profile of the valence band upward from the Si side, indicating a decrease of the barrier height [20].

A typical dark current–voltage (I–V) plot of the Au/Fe(III)ClTPP/p-Si/Al heterojunction device at room temperature for the as-fabricated device and for the irradiated one by γ-irradiation with doses of 1 and 1.25 kGy is shown in figure 7. This device exhibits a diode behavior. The forward bias direction corresponds to the situation when the Au electrode is positive. The current–voltage characteristics of the device exposed to γ-irradiation shifted toward the high-voltage side in comparison with that before irradiation. The current in the forward and reverse bias directions decreases with increasing the irradiation dose; this

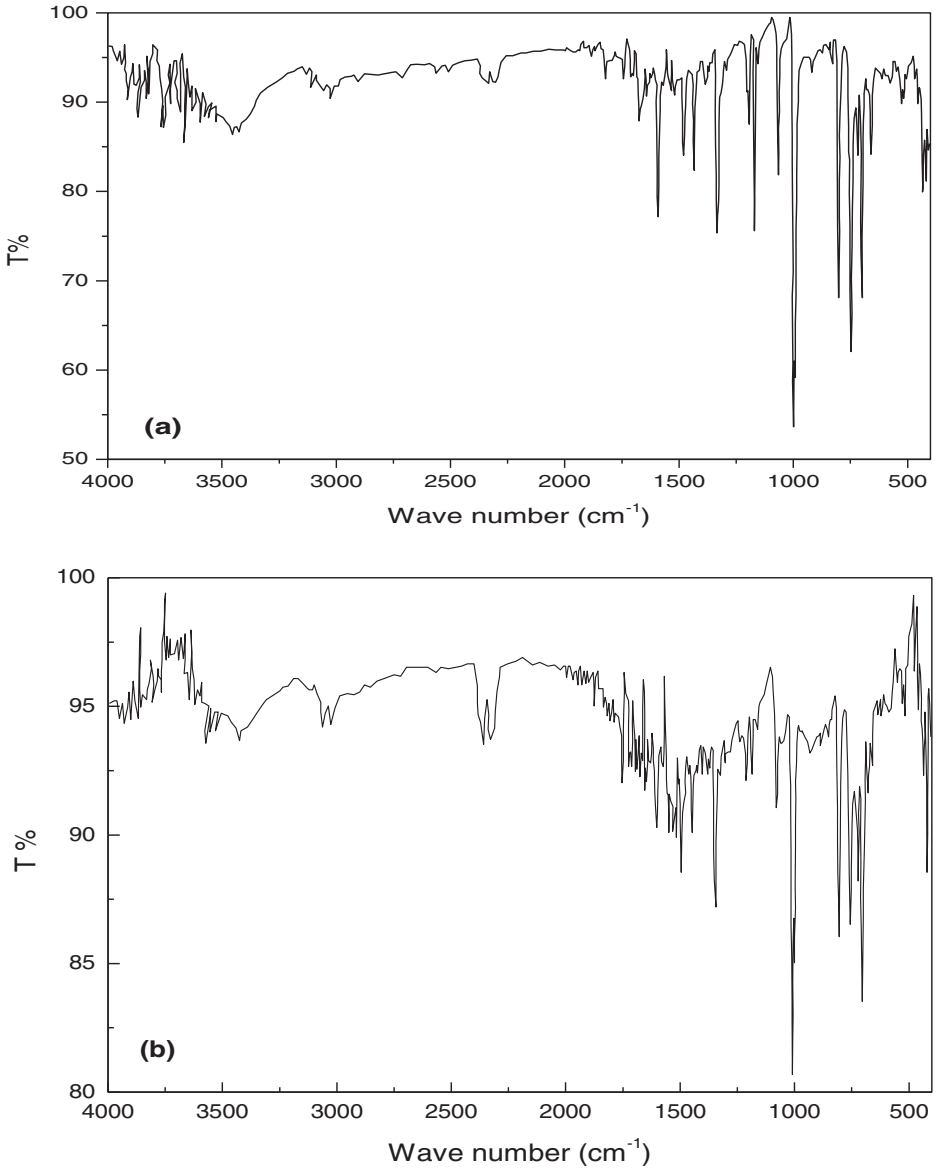

Figure 3. FTIR spectra of Fe(III)ClTPP: (a) in powder form and (b) as deposited thin films.

Table 1. Assignment of transmission bands for Fe(III)ClTPP in powder form and in thin film conditions.

Fe(III) Cl TPP conditions		
Powder	As deposited thin film	
Wave number, cm^{-1}		Assignment
3445.21	3420.14	N–H stretch in phenyl
3057.58	3053.73	C–H stretch in porphyrin
1590.99	1595.81	C=C stretch in phenyl
1443.46	1439.6	C–H bend in phenyl
1170.58	1179.26	C–H bend in phenyl
1071.26	1073.19	C–H bend, complex
997.982	996.053	In-plane bending in porphyrin
875.524	878.417	C–H out-of-plane in porphyrin
841.776	844.669	C–H out-of-plane of phenyl
802.242	801.278	C–H out-of-plane in porphyrin
701.962	703.89	Out-of-plane deformation of phenyl
657.607	657.607	In-plane vibration deformation porphyrin
618.074	621.931	Out-of-plane deformation porphyrin

can be attributed to the increase in the interfacial defect density [21]. The values of the rectification ratio (RR) at ±1 V was calculated for as-fabricated and irradiated devices and displayed in table 3. The series and shunt resistances R_s and R_{sh}, respectively, were determined by plotting the junction resistance R_j as the ordinate and bias potential as the abscissa

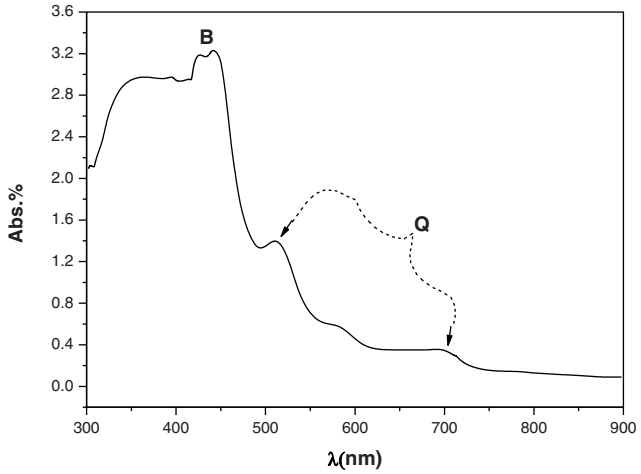

Figure 4. Absorbance spectra of Fe(III)ClTPP thin films.

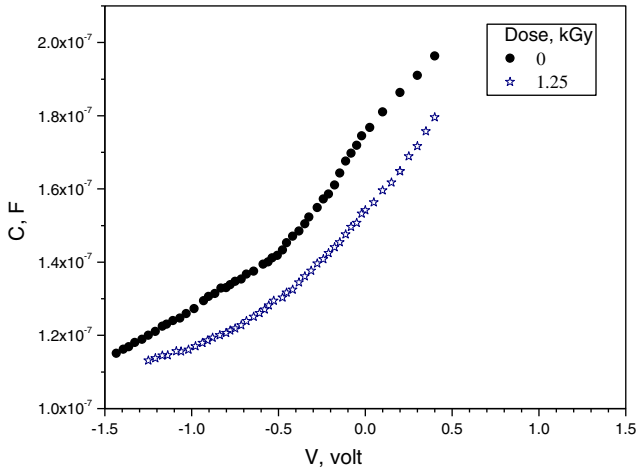

Figure 5. Plot of the *C*–*V* characteristics of the Au/Fe(III)ClTPP/p-Si/Al device before and after γ-irradiation.

Table 2. Variation of *C*–*V* parameters with irradiation dose for the Au/Fe(III)ClTPP/p-Si/ Al heterojunction device.

Dose, kGy	$C_{Jo} \times 10^{-7}$ F cm^{-2}	V_{bi}, V	$N_S \times 10^{12}$, m^{-3}
0	1.75	0.4	11
1.25	1.54	0.77	10

Table 3. Dose-dependent values of various parameters determined from *I*–*V* characteristics of the Au/Fe(III)ClTPP/p-Si/Al heterojunction device.

Dose, kGy	0	1	1.25
RR	4.16	3.95	4.43
I_o (A)	8.17×10^{-7}	5.2×10^{-7}	1.57×10^{-7}
ξ	5.9	6.55	4.3
φ_b(eV)	0.41	0.42	0.45

as illustrated in figure 8. R_j is determined [7] as

$$R_j = \frac{\partial V}{\partial I}. \quad (2)$$

Figure 8 shows that R_j decreases with increasing the forward bias potential. At high forward bias potentials, the junction resistance arrives at a constant value of series resistance, which is 1.3 kΩ for the unirradiated device, 3.5

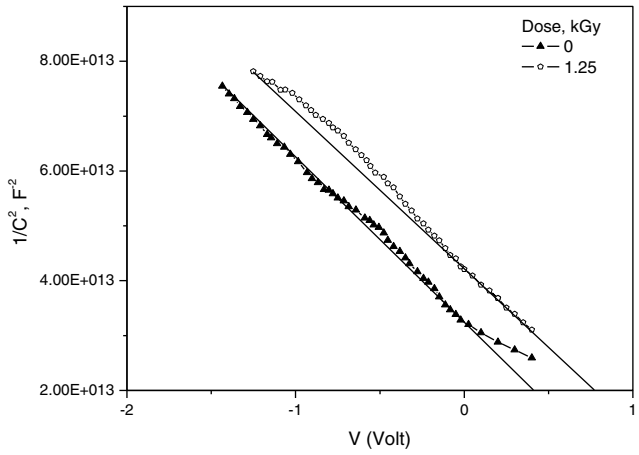

Figure 6. Plot of $1/C_j^2$ versus potential for as-fabricated and γ-irradiated Au/Fe(III)ClTPP/p-Si/Al devices.

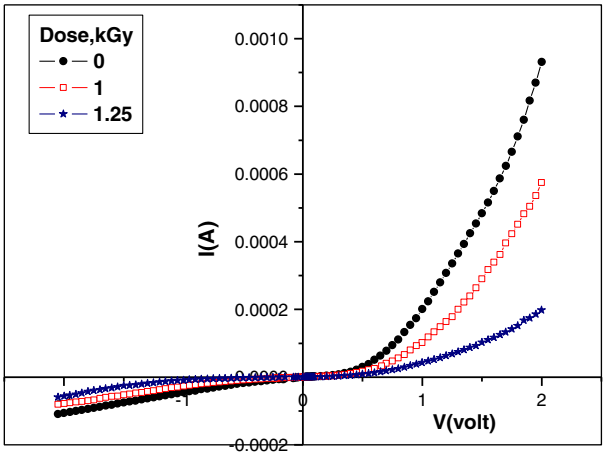

Figure 7. Dark *I*–*V* characteristics for as-fabricated and γ-irradiated Au/Fe(III)ClTPP/p-Si/Al heterojunction devices at room temperature ($T = 298$ K).

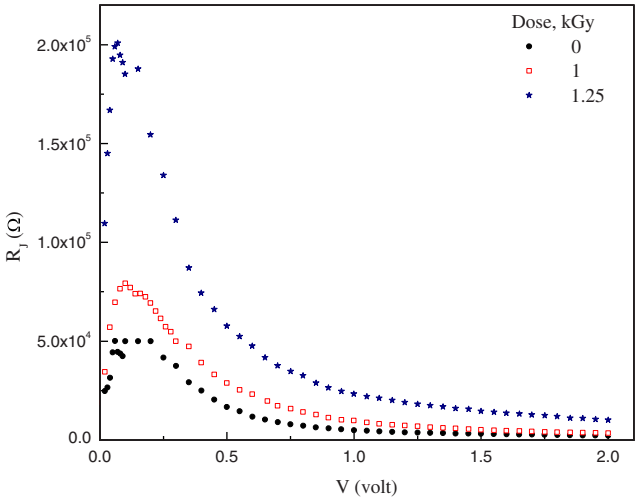

Figure 8. The junction resistance (R_j) as a function of potential bias (V).

and 10.7 kΩ for the irradiated device with doses, 1 and 1.25 kGy, respectively. The maximum value of R_s occurs at about 0.06–0.2 V. These peaks shifted to the accumulated region with increasing the irradiation dose. This behavior

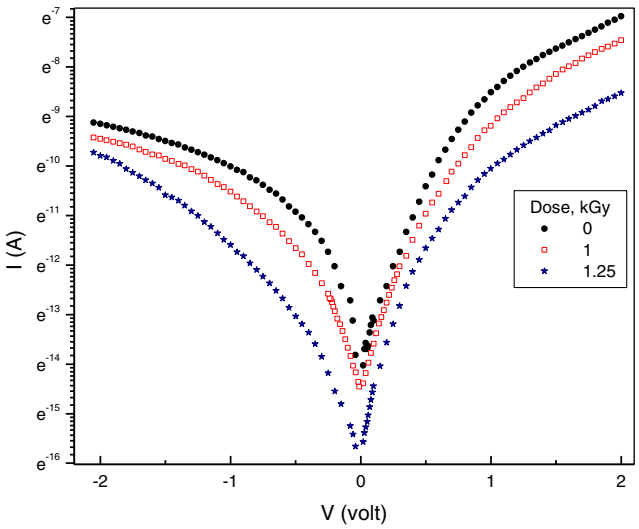

Figure 9. Dark ln *I–V* characteristics for as-fabricated and γ-irradiated Au/Fe(III)ClTPP/p-Si/Al heterojunction devices at room temperature ($T = 298$ K).

of junction resistance has been attributed to a particular distribution of interface states [22]. Such a behavior of junction resistance with voltage and irradiation doses has been observed in Sn/p-Si Schottky barrier diodes [23] and ZnO/n-Si device [24].

The *I–V* characteristics in the forward current direction can be classified into two regions depending on the applied voltage. This behavior indicates the presence of two conduction mechanisms. Firstly, the current increases exponentially up to $V < 0.6$ V as shown in figure 9 and this indicates that thermionic emission is the operating conduction mechanism in that potential region. The current is related to the potential in this region by [18]

$$I = I_o\left[\exp\frac{q(V - IR_s)}{\xi k_B T} - 1\right] + \frac{V - IR_s}{R_{sh}}, \tag{3}$$

where ξ is the diode quality factor, which must be equal to 1 in the case of ideal diode, T is the absolute temperature and I_o is the saturation current, which is given by [18]

$$I_o = AA^*T^2\exp(-q\varphi_{bo}/k_B T), \tag{4}$$

where A is the effective area of the device and is equal to 0.2 cm^2, A^* is the Richardson constant (32 A cm^{-2} K^2 for p-type Si [18]), φ_{bo} is the zero bias barrier height at the interface of the Fe(III)ClTPP/p-Si heterojunction device and k_B is the Boltzmann constant. From equations (3) and (4), the ideality factor, ξ, and barrier height, φ_{bo}, can be written, respectively, as

$$\xi = \frac{q}{k_B T}\frac{dV}{d\ln(I)} \tag{5}$$

and

$$\varphi_{bo} = \frac{k_B T}{q}\ln\left(\frac{AA^*T^2}{I_o}\right). \tag{6}$$

Figure 9 shows a plot of the logarithmic current as a function of the bias voltage. The saturation current and the diode quality factor can be obtained from the intercept with the ordinate axis and the slope of the curve in the thermionic conduction region, respectively. Table 3 illustrates the ξ, I_o and φ_{bo} values determined from *I–V* characteristic curves of the Au/Fe(III)ClTPP/p-Si/Al heterojunction device. The ideality factor for the as-manufactured device is greater than unity, showing the deviation from ideal diode properties. This can be ascribed to the barrier height inhomogeneity resulting from the presence of a very thin oxide layer between the metal and the semiconductor [25] or the presence of conduction mechanisms such as recombination-generation, tunnelling and image-force effects [26]. It was found that diode quality factor varies with irradiation doses, and irradiating a device with a dose of 1.25 kGy reduces the ξ value to 4.33; this is due to inhomogeneity of the interface that depends upon γ-irradiation-induced damage [26].

The voltage-dependent ideality factor $\xi(V)$ and the interface states density, N_{ss}, can be expressed [27] as follows:

$$\frac{1}{\xi(V)} = \frac{\varepsilon_i}{\varepsilon_i + q^2 N_{ss}\delta}, \tag{7}$$

where ε_i is the permittivity of the interfacial layer and is equal to $4\varepsilon_o$ [22] and δ is the thickness of the interfacial layer. The quality factor voltage dependence is given by

$$\xi(V) = \frac{V}{(k_B T/q)\mathrm{Ln}(I/I_o)}. \tag{8}$$

The applied voltage dependence of the barrier height is given as

$$\varphi_c = \varphi_b + \beta V, \tag{9}$$

where β is the voltage coefficient of the effective barrier height, φ_c. Differentiating the effective barrier height, φ_c, with respect to applied voltage V results in a parameter that combines the effects of the interface states energy, E_{ss}, and interfacial layer thickness [22] as follows:

$$\frac{d\varphi_c}{dV} = \beta = 1 - \frac{1}{\xi(V)}. \tag{10}$$

The energy of interface states in a p-type semiconductor is given as [19]

$$E_{ss} - E_v = q(\varphi_c - V), \tag{11}$$

where E_v is the top energy of valence band. N_{ss} can be calculated by substituting voltage-dependent values and other parameters in equation (7); the N_{ss} versus $E_{ss} - E_v$ is depicted in figure 10. N_{ss} for as-manufactured Au/Fe(III)Cl TPP/p-Si/Al heterojunction device increases nonlinearly with bias from 4.71×10^{10} cm^{-2} eV^{-1} at $(0.63 - E_v)$ eV to 3.98×10^{11} cm^{-2} eV^{-1} at $(0.43 - E_v)$ eV. Also N_{ss} for the irradiated Au/Fe(III)Cl TPP/p-Si/Al device increases nonlinearly with bias from 1.75×10^{11} cm^{-2} eV^{-1} at $(0.65 - E_v)$ eV to 4.22×10^{11} cm^{-2} eV^{-1} at $(0.46 - E_v)$ eV. The increase of N_{ss} with irradiation dose elucidates the decrease of current in the forward and reverse bias directions with an increase of irradiation dose.

The saturation current decreased from 8.12×10^{-7} A for the as-fabricated device to 1.7×10^{-7} A for the irradiated device with a dose of 1.25 kGy. El-Nahass *et al* [9] showed that for Fe(III)Cl TPP the width of the tail of localized states in the forbidden band gap increases by irradiation and the

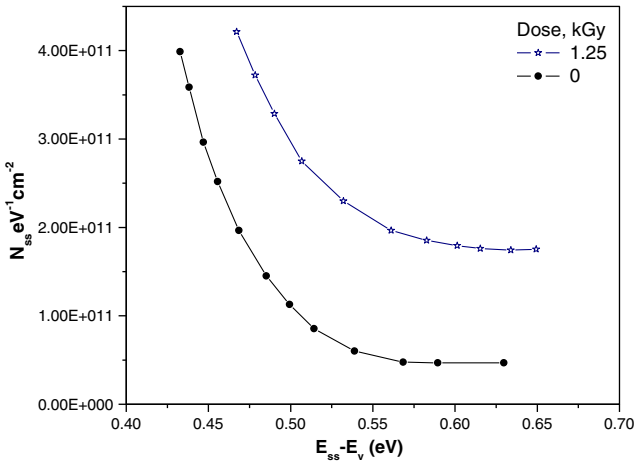

Figure 10. Plot of N_{ss} versus (E_{ss}–E_v) for the Au/Fe(III)ClTPP/p-Si/Al heterojunction device.

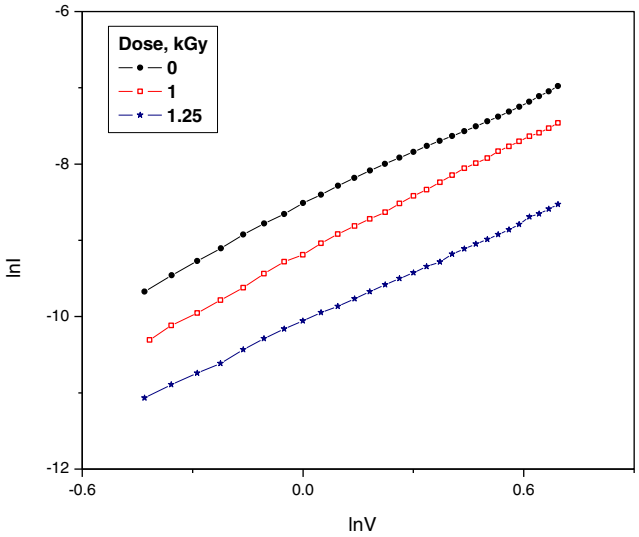

Figure 11. Dark ln I–ln V characteristics for as-fabricated and γ-irradiated Au/Fe(III)ClTPP/p-Si/Al heterojunction devices at room temperature ($T = 298$ K).

excitonic and trap levels are also affected by irradiation. The decrease in reverse current after γ-irradiation is due to deep level traps in the band gap that act as the recombination center and reduces the reverse current [14]. The recombination centers are considered a reason for the increasing of ideality factor upon irradiation [26].

The barrier height of the device increased from 0.41 eV for the as-fabricated device to 0.45 eV for the γ-irradiated device. The increase in barrier height of some devices such as the Sn/p-Si diode [25] and methyl violet/p-Si diode [28] with γ-ray irradiation doses has been reported. The decrease of carrier concentration in the depletion region due to the occurrence of traps and recombination center resulting from irradiation damage as shown in table 2 is considered to be a reason for the increasing potential barrier height [28].

In the voltage region ($V > 0.6$ V), the current shows a power dependence on voltage, i.e. it follows the relation $I \sim V^m$, where m ranges from 2.22 to 2.25 depending on irradiation dose taken from the slope of the Ln I–Ln V plot which is shown in figure 11. This square power dependence suggests that the current is an SCLC with single-level

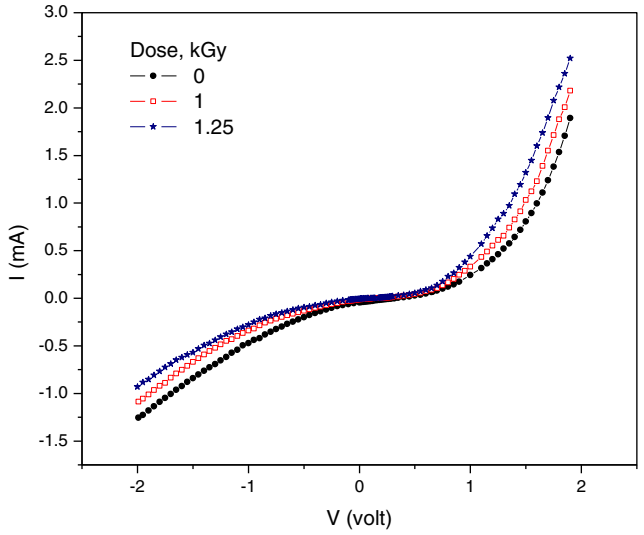

Figure 12. I–V characteristic curve for as-fabricated and γ-irradiated Au/p-Fe(III)ClTPP/p-Si/Al heterojunction devices under illumination and at room temperature ($T = 298$ K).

distribution of traps, which is given by [29]

$$I_{\mathrm{SCLC}} = \frac{9}{8} A \varepsilon_o \varepsilon_r \mu \frac{V^2}{d^3}, \tag{12}$$

where ε_r is the relative permittivity of the organic compound, μ is the carrier mobility and d is the film thickness.

The photovoltaic response of the Au/Fe(III)ClTPP/p-Si/Al sensor under illumination through the Au electrode is depicted in figure 12. The I–V measurements of the sensor were measured at room temperature for the as-fabricated device and for those devices after being irradiated with doses of 1 and 1.25 kGy. In contrast to the dark current–voltage characteristics shown in figure 7, the photocurrent in the forward bias direction increases with an increase in irradiation dose. γ-irradiation induces defects in the band gap, which affect the free carrier's concentration [30], and electrically active defects are created in the energy gap which act as traps or as recombination centers in the semiconductors [31] and the generation of excess electronic localized states in the gap of a semiconductor [32]. All these defects decrease the energy gap of a semiconductor and therefore increase the photocurrent.

4. Conclusions

The study of γ-irradiation doses on the electrical parameters of an Au/Fe(III)ClTPP/p-Si/Al heterojunction diode indicates that irradiation induces defect states in the interfacial layer and energy gap of a semiconductor. As a result, the parameters of C–V and I–V characteristics were found to be influenced by irradiation dose. The capacitance at zero bias potential and carrier density in the depletion region decrease with an increase in irradiation dose. The density of defect states in the interfacial layer and in the energy gap of a semiconductor increase with irradiation dose. The irradiation dose increases the value of the series resistance, built-in potential and rectification ratio. The ideality factor depends on the irradiation dose. The variation of the C–V and I–V parameters of the Au/Fe(III)ClTPP/p-Si/Al diode shows that this device may have application as a γ-ray sensor.

References

[1] Campbell I H, Rubin S, Zawodeinski T A, Kress J D, Martin R L, Smith D L, Barashkov N N and Ferraris J P 1996 *Phys. Rev.* B **54** R14321–4

[2] Zhang X Q, Wu H M, Wei Y, Cheng Z P and Wu X J 1995 *Solid State Commun.* **95** 99–101

[3] Zhang X Q, Wu H M, Wu X J, Cheng Z P and Wei Y 1995 *J. Mater. Chem.* **5** 401–4

[4] Tonezzer M, Quaranta A, Maggioui G, carturan S and Mea G D 2007 *Sensors Actuators* B **122** 620–6

[5] Gryko D T, Clausen C and Lindseg J S 1999 *J. Org. Chem.* **64** 8635–47

[6] Umeyama T, Takamatsu T, Tezuka N, Matano Y, Araki Y, Wada T, Yoshikawa O, Sagawa T, Yoshikawa S and Imahori H 2009 *J. Phys. Chem.* C **113** 10798–806

[7] El-Nahass M M, Zeyada H M, Aziz M S and Makhlouf M M 2005 *Thin Solid Films* **492** 290–7

[8] Wagner R W and Lindsey J S 1994 *J. Am. Chem.* **116** 9759–60

[9] El-Nahass M M, El-Deeb A F, Metwally H S, El-Sayed H E A and Hassanien A M 2010 *Solid State Sci.* **12** 552–7

[10] El-Nahass M M, El-Deeb A F, Metwally H S and Hassanien A M 2011 *Mater. Chem. Phys.* **125** 247–51

[11] Farag A A M and Yahia I S 2010 *Opt. Commun.* **283** 4310–17

[12] Auret F D, Goodman S A, Erasmus R, Meyer W E and Myburg G 1995 *Nucl. Instrum. Methods* B **106** 323–7

[13] Dharmarsu N, Arulkumaran S, Sumathi R R, Jayavel P, Kumar J, Magudapathy P and Nair K G M 1998 *Nucl. Instrum. Methods* B **140** 119–23

[14] Mamor M, Sellai A, Bauziane K, Al Harthi S H, Al Busaidi M and Gard F S 2007 *J. Phys. D: Appl. Phys.* **40** 1351–6

[15] Gutmann F and Lyons L E 1981 *Organic Semiconductors A* (Malabar, FL: Krieger)

[16] Tolansky S 1970 *Multiple-Beam Interference Microscopy of Metals* (London: Academic)

[17] Gonzalez P, Serra J, Chiussi S, Leon B and Perez-Amor M 2003 *J. Non-Cryst. Solids* **320** pp 92–9

[18] Sze S M 1969 *Physics of Semiconductor Devices* (New York: Wiley)

[19] El-Nahass M M, Metwally H S, El-Sayed H E A and Hassanien A M 2011 *Synth. Met.* **161** pp 2253–58

[20] Pandy S and Kal S 1998 *Solid-State Electron.* **42** 943–49

[21] Tataroglu A, Altindal S and Bülbül M M 2006 *Nucl. Instrum. Methods* A **568** 863–8

[22] Rhoderick E H and Williams R H 1988 *Metal–Semiconductor Contacts* 2nd edn (Oxford: Clarendon)

[23] Karatas S and Türüt A 2006 *Nucl. Instrum. Methods* A **566** 584–9

[24] Ocak Y S, Kiliçoğlu T, Topal G and Başkan M H 2010 *Nucl. Instrum. Methods* A **612** 360–6

[25] Karatas S, Türüt A and Altindal S 2005 *Nucl. Instrum. Methods* A **555** 260–5

[26] Jayavel P, Kumar J, Santhakumar K, Magudapathy P and Nair K G M 2000 *Vacuum* **57** 51–9

[27] Cowley A M and Sze S M 1965 *J. Appl. Phys.* **36** 3212–20

[28] Güllü Ö, Çankaya M, Biber M and Türüt A 2008 *J. Phys. D: Appl. Phys.* **41** 135103

[29] Ahmed A and Collins R A 1991 *Phys. Status Solidi* a **123** 201–11

[30] Fonash S J, Ashok S and Singh R 1981 *Appl. Phys. Lett.* **39** 423–9

[31] Jayavel P, Udhayasankar M, Kumar J, Asokan K and Kahjilal D 1999 *Nucl. Instrum. Methods* B **156** 110–15

[32] El-Sayed S M 2004 *Nucl. Instrum. Methods* B **225** 535–43